HHS Public Access

Author manuscript

*Am J Surg Pathol*. Author manuscript; available in PMC 2021 April 01.

Published in final edited form as:

*Am J Surg Pathol*. 2018 March ; 42(3): 279–292. doi:10.1097/PAS.0000000000001000.

# Reappraisal of Morphological Differences between Renal Medullary Carcinoma, Collecting Duct Carcinoma, and Fumarate Hydratase-Deficient Renal Cell Carcinoma

**Chisato Ohe, MD**[1], **Steven C. Smith, MD, PhD**[2], **Deepika Sirohi, MD**[1], **Mukul Divatia, MD**[3], **Mariza de Peralta-Venturina, MD**[1], **Gladell P. Paner, MD**[4], **Abbas Agaimy, MD**[5], **Mitual B. Amin, MD**[6], **Pedram Argani, MD**[7], **Ying-Bei Chen, MD, PhD**[8], **Liang Cheng, MD**[9], **Maurizio Colecchia, MD**[10], **Eva Compérat, MD, PhD**[11], **Isabela Werneck da Cunha, MD, PhD**[12], **Jonathan I. Epstein, MD**[7], **Anthony J. Gill, MD, FRCPA**[13], **Ondřej Hes, MD, PhD**[14], **Michelle Hirsch, MD, PhD**[15], **Wolfram Jochum, MD**[16], **Lakshmi P. Kunju, MD**[17], **Fiona Maclean, FRCPA**[18], **Cristina Magi-Galluzzi, MD, PhD**[19], **Jesse K. McKenney, MD**[19], **Rohit Mehra, MD**[17], **Gabriella Nesi, MD**[20], **Adeboye O. Osunkoya, MD**[21], **Maria M. Picken, MD, PhD**[22], **Priya Rao, MD**[23], **Victor E. Reuter, MD**[8], **Paulo Guilherme de Oliveira Salles, MD**[24], **Luciana Schultz, MD**[25], **Satish K. Tickoo, MD**[8], **Scott A. Tomlins, MD, PhD**[17], **Kiril Trpkov, MD, FRCPC**[26], **Mahul B. Amin, MD.**[1,27]

[1]Department of Pathology and Laboratory Medicine, Cedars-Sinai Medical Center, Los Angeles, CA [2]Departments of Pathology and Urology, VCU School of Medicine, Richmond, VA USA [3]Department of Pathology, Houston Methodist Hospital, Weill Medical College of Cornell University, Houston [4]Department of Pathology, University of Chicago, Chicago, IL [5]Institute of Pathology, Friedrich-Alexander-University, Erlangen, Germany [6]William Beaumont Hospital, Royal Oak, MI [7]Johns Hopkins Hospital, Baltimore, MD [8]Memorial Sloan Kettering Cancer Center, New York, NY [9]Indiana University School of Medicine, Indianapolis, IN [10]Fondazione IRCCS Istituto Nazionale dei Tumori, Milan, Italy [11]Groupe Hospitalier Pitié-Salpêtrière, Université Pierre et Marie Curie, Paris, France [12]Department of Pathology, AC Camargo Cancer Center, São Paulo, Brazil [13]Cancer Diagnosis and Pathology Group, Kolling Institute of Medical Research Royal North Shore Hospital and University of Sydney, Sydney, Australia [14]Charles University Hospital, Pilsen, Czech Republic [15]Brigham and Women's Hospital, Boston, MA [16]Katonsspital St Gallen, St Gallen, Switzerland [17]University of Michigan, Ann Arbor, MI [18]Douglass Hanly Moir Pathology, Sydney, Australia [19]Pathology and Laboratory Medicine Institute, Cleveland Clinic, Cleveland, OH [20]Carregi Hospital, Florence, Italy [21]Emory University School of Medicine, Atlanta, GA [22]Department of Pathology, Loyola University, Maywood, IL [23]MD Anderson Cancer Center, Huston, TX [24]Associacao Mario Penna, Hospital Luxemburgo, Belo Horizonte-MG, Brazil [25]Instituto de Anatomia Patologica, Piracicaba, Brazil [26]Calgary Laboratory Services and University of Calgary, AB, Canada [27]Department of Pathology and Laboratory Medicine and Urology, University of Tennessee Health Science Center, Memphis, TN, USA

Correspondence: Mahul B. Amin, MD, Professor and Chairman, Department of Pathology and Laboratory Medicine, University of Tennessee Health Science Center, 930 Madison Avenue; Suite 531, Memphis, TN 38163, (901) 448-7020 (office), (901) 448-1876 (fax, mamin5@uthsc.edu.

## Abstract

Renal Medullary Carcinomas (RMCs) and Collecting Duct Carcinomas (CDCs) are rare subsets of lethal high-stage, high-grade distal nephron-related adenocarcinomas with a predilection for the renal medullary region. Recent findings have established an emerging group of fumarate hydratase (FH)-deficient tumors related to hereditary leiomyomatosis and renal cell carcinoma syndrome (HLRCC-RCCs) within this morphologic spectrum. Recently-developed, reliable ancillary testing has enabled consistent separation between these tumor types. Here, we present the clinicopathologic features and differences in the morphological patterns between RMCs, CDCs and FH-deficient RCCs in consequence of these recent developments. This study included a total of 100 cases classified using contemporary criteria and ancillary tests. Thirty-three RMCs (SMARCB1/INI1-deficient, hemoglobinopathy), 38 CDCs (SMARCB1/INI1-retained) and 29 RCCs defined by the FH-deficient phenotype (FH-/2SC+ or FH±/2SC+ with *FH* mutation, regardless of HLRCC syndromic stigmata/ history) were selected. The spectrum of morphologic patterns was critically evaluated and the differences between the morphological patterns present in the three groups were analyzed statistically. Twenty five percent of cases initially diagnosed as CDC were reclassified as FH-deficient RCC based on our contemporary diagnostic approach. Among the different overlapping morphologic patterns, sieve-like/cribriform and reticular/yolk sac tumor-like patterns favored RMCs, whereas intracystic papillary and tubulocystic patterns favored FH-deficient RCC. Tubulopapillary pattern favored both CDCs and FH-deficient RCCs, and multinodular infiltrating papillary pattern favored CDCs. Infiltrating glandular and solid sheets/ cords/nested patterns were not statistically different among the three groups. Viral inclusion-like large nucleoli considered as a hallmark of HLRCC-RCCs were observed significantly more frequently in FH-deficient RCCs. Despite the overlapping morphology found among these clinically aggressive infiltrating high-grade adenocarcinomas of the kidney, reproducible differences in morphology emerged between these categories after rigorous characterization. Finally, we recommend that definitive diagnosis of CDC should only be made if RMC and FH-deficient RCC are excluded.

### Keywords

renal medullary carcinoma; collecting duct carcinoma; FH-deficient renal cell carcinoma; hereditary leiomyomatosis and renal cell carcinoma syndrome associated renal cell carcinoma; morphology

## Introduction

Renal medullary carcinomas (RMCs)[1–5] and collecting duct carcinomas (CDCs)[5–8] are rare subsets of high-grade, usually high-stage lethal renal tumors putatively of distal nephron derivation with a predilection for the renal medullary region. We herein designate these groups of tumors as ‘high-grade distal nephron-related adenocarcinomas’, which we have designated HDNAs, which are morphologically characterized by an infiltrating adenocarcinoma within a desmoplastic stroma (after exclusion of metastases and glandular upper tract urothelial carcinoma).

Based on recent findings, we have come to consider an emerging group of fumarate hydratase (FH)-deficient renal cell carcinomas, related to Hereditary Leiomyomatosis-Renal Cell Carcinoma syndrome (HLRCC-RCCs), to potentially overlap with the morphological spectrum of high grade distal nephron-related adenocarcinomas.[9,10] HLRCC-RCCs occur in the setting of cutaneous and/or uterine leiomyomatosis,[11–14] and require the presence of *FH* germline mutations for a definitive diagnosis.[15–17] On the other hand, we have proposed the diagnostic term *FH-deficient RCC* for those tumors showing FH-deficiency (by IHC and/or tumor mutation profiling) in the setting of absent or uncertain clinical history of HLRCC and germline status.[18] A combined immunohistochemical (IHC) approach of FH loss and induction of aberrant modification of cellular proteins with S-(2-succino)-cysteine (2SC) or *FH* mutation analysis are useful diagnostic tools in ascertaining FH-deficient status of these tumors.[9,10,19,20] Most recently, several of us demonstrated that HLRCC-RCCs and FH-deficient RCCs share remarkable clinicopathologic similarities,[9,10] and on histology displayed admixed architectural patterns such as papillary, tubular, solid, cribriform and tubulocystic, and small and medium gland infiltrative adenocarcinoma pattern, with invariable presence of viral inclusion-like macronucleoli. [9,10,19] Importantly, many of these features and architectural patterns overlap with those seen in the aforementioned HDNAs, despite the lack of evidence (we acknowledge) relating FH-deficient RCCs to the distal nephron. However, the morphological patterns have not been previously studied comprehensively across this spectrum of high grade distal nephron-related adenocarcinoma categories, and it remains unclear whether specific morphologic features are of use in the differential diagnosis.

In this study, we classified a group of tumors in the morphologic range that is associated with high grade distal nephron-related adenocarcinomas into RMCs, CDCs, and FH-deficient RCCs (including both proven HLRCC-RCCs and RCCs defined only by the immunophenotype and/or confirmation of *FH* mutation) after rigorous clinicopathologic and IHC correlation. Our goal was to ascertain whether differential histopathologic features, particularly growth patterns, can assist in triage of work-up and histological classification of these rare but often lethal renal tumors.

## MATERIAL AND METHODS

### Case selection

We invited several collaborators to contribute cases that they regarded as in the morphologic spectrum associated with high grade distal nephron-related adenocarcinomas for a comprehensive morphologic, immunohistochemical, and clinicopathologic review. We received 121 cases from 27 contributors. Since the aim of this effort was to perform a series of studies related to these rare tumors, for academic purposes and to maintain continuity, we designated this group of collaborators as the “High-grade Distal Nephron-related Adenocarcinoma International Consortium”. It included contributors from 25 international institutions from 10 countries, many of them representing large uropathology practices with broad referral and consultation bases. Thirty-eight previously published cases were also included in this study.[7,9,10,21] The study was approved by respective Institutional Review Boards of each institution. The number of hematoxylin and eosin (H&E) slides available for

study review ranged from 1 to 26 slides per case (mean 4.2). Available clinical, follow-up, and macroscopic data were tabulated and histological slides were reviewed by three authors (C.O./D.S./M.B.A.). The renal tumors were classified into three categories using stringent contemporary criteria [4,5,8,17,19] and ancillary tests as follows (also outlined in Fig. 1):

i) The diagnosis of RMC was confirmed by hemoglobinopathy (sickle cell trait or related hemoglobinopathies and/or finding sickled erythrocytes in the histological samples) and complete loss of SMARCB1 (INI1) expression by IHC. We excluded RCC, unclassified RCC with medullary phenotype, representing tumors morphologically similar to RMCs, but lacking the evidence of hemoglobinopathy (n=4).[1–5,22]

ii) The diagnosis of CDC was defined using the recently described criteria,[4,5,7,22]; which required exclusion of RMC, FH-deficient RCC, urothelial carcinomas of the upper tract and metastatic carcinomas.

iii) FH-deficient RCC was diagnosed based on IHC evidence of FH loss and 2SC positivity and/or confirmation of *FH* mutation, regardless of the presence or absence of HLRCC syndromic history or stigmata.[9,10,19] In this study, we used the FH-deficient term as a unifying term to describe the spectrum of tumors that includes bona fide HLRCC, confirmed by germline mutation and with HLRCC stigmata/history as well as FH-deficient RCCs defined by lack of IHC expression of FH and induction of 2SC positivity without a history of HLRCC in a morphologically appropriate tumor. FH-suspicious RCCs which showed equivocal FH and 2SC positive results with unknown *FH* mutation status were excluded from this group (n=7). The remaining 10 cases did not fit into these diagnostic categories and were excluded from this cohort.

## Histology and Immunohistochemistry

To compare the morphologic patterns amongst high grade distal nephron-related adenocarcinoma categories, H&E stained sections were evaluated using eight morphological patterns, similar to our prior study[10]; 1) infiltrating glandular pattern of small or medium sized elongated tubules in a desmoplastic stroma, 2) multinodular infiltrating papillary pattern, 3) tubular/tubulopapillary/papillary pattern, 4) solid sheets/cords/nested pattern and/or rhabdoid features, 5) intracystic papillary pattern with or without hyalinized cores, 6) sieve-like/cribriform pattern, 7) tubulocystic carcinoma-like pattern and 8) reticular/yolk sac tumor (YST)-like pattern. Morphological patterns were assigned scores from 0–3 based on a quantitative approach. Score 3 was assigned to the primary pattern occupying ≥ 50% of the tumor, score 2 to the secondary pattern occupying 11%−49%, score 1 to tertiary pattern occupying ≤10%, and score 0 when the pattern was lacking. Scores 1–3 were considered positive. Viral inclusion-like eosinophilic nucleoli with perinucleolar halos, a hallmark of HLRCC-RCCs, were scored as: 2+ = diffuse, 1+ = focal, and 0 = absent. Additionally, presence or absence of coagulative tumor necrosis, dysplastic in situ changes in adjacent renal tubules, stromal myxoid change and sarcomatoid changes were also assessed. Evaluation of the nucleolar grade was based on the ISUP 2012 criteria,[23] endorsed by the World Health Organization (WHO) (ISUP/WHO nucleolar grade).

### Statistical analysis

Clinico-pathological features of RMCs, CDCs, and FH-deficient RCCs were statistically analyzed using the chi-square test, and $p$-value < 0.0167 was considered significant among the 3 groups based on the Bonferroni's method. Age and tumor size were analyzed by the Kruskal-Wallis test, and $p$-value < 0.05 was considered significant. Any parameter significantly different between the 3 groups was subsequently analyzed between pairs of subtypes, using the chi-square test, and considering a $p$-value < 0.05 to be significant.

### Immunohistochemistry

IHC staining was performed using primary antibodies to PAX8 (polyclonal; predilute; Cell Marque, Rocklin, CA), S100A1 (EPR5250; 1:1500: Abcam, Cambridge, MA), SMARCB1/INI1 (MRQ-27; predilute; Cell Marque), and OCT3/4 (MRQ10; predilute; Cell Marque) following the manufacturer's protocols with appropriate positive and negative controls. Immunoreactivity was scored as 0–3+ based on the percentage of positive tumor cells (0; 0%, 1+; <10%, 2+; 10–50%, 3+; >50%). Scores 1–3 were considered positive results.

FH immunostaining was performed on all cases at two institutions using anti-FH mouse monoclonal antibody (clone J-13, Santa Cruz Biotechnology, USA) as reported previously.[9,10] The stain was evaluated qualitatively as positive or negative compared to the internal control within the tumor. FH staining was recorded as following; retained: +, equivocal: ±, complete loss: –.

Due to limited availability of 2SC antibody, the stain was performed on selected cases that were FH-, FH±, or morphologically highly suspicious for HLRCC-RCC. 2SC staining was performed in two laboratories using polyclonal antibody following the method previously described.[9,10,19] The stain was assessed for intensity (1+ to 3+) and only nucleocytoplasmic staining with 3+ intensity was considered positive.[10,19]

## RESULTS

### Clinical Features

The clinical data for RMCs, CDCs and FH-deficient RCCs are summarized in Table 1. Briefly, patient age was statistically different amongst the three groups ($p<<0.001$) with median ages of 27.0, 65.5, and 45.0, respectively. There was a male predilection in all tumor types with male to female ratio ranging from 2.6:1 to 3.2:1. RMCs predominantly occurred in African Americans (78%: 25/32) with a smaller portion in Caucasians (9%: 3/32) and other ethnicities (French Guinean, Hispanic, and Saudi Arabian), whereas CDCs and FH-deficient RCCs were more common in Caucasians (90%: 28/31 and 71%: 17/24, respectively). Sickle cell disorder was seen only in RMCs as per selection criteria: 82% (27/33) of the patients had documented sickle cell hemoglobinopathy, and in the remaining 18% (6/33) where sickle cell trait or hemoglobinopathy history was unavailable, sickled erythrocytes were diffusely present on histological examination. HLRCC syndromic history or stigmata were only evident in FH-deficient RCCs: 39% (7/18) of the patients had family history of HLRCC syndrome or RCC, and 29% (5/17) had cutaneous or uterine leiomyomas.

There was a predilection for the right kidney in RMCs ($p$=0.0138). The tumors in all subtypes were large, with mean size ranging from 6.3 cm to 8.5 cm.

Stage category pT3 or higher was seen in 85% (27/33), 91% (31/34), and 75% (21/28) cases of RMC, CDC, and FH-deficient RCC, respectively. Regional lymph node metastasis was more prevalent, at 96% (25/26) in RMC, *versus* 48% (13/27) in CDC and 58% (15/26) in FH-deficient RCC ($p$<0.0167). Systemic metastases were frequent in all categories: 94% (30/32) in RMC (70%; 19/27 at presentation), 73% (16/22) in CDC (47%; 7/15 at presentation), and 65% (17/26) in FH-deficient RCC (46%; 6/13 at presentation). Frequent metastatic sites were lung (n=21), liver (n=12) and bone (n=7) in RMCs; lung (n=10), bone (n=7) and brain (n=3) in CDC; liver (n=9), lung (n=6) and bone (n=5) in FH-deficient RCC. Disease related fatal outcomes were documented in 83% (24/29) of RMC cases, and in 61% (14/23) of both CDC and FH-deficient RCC. As described previously,[9,10] 14 of FH-deficient RCCs were confirmed by sequencing data, including 4 *FH* mutations confirmed by germline sequencing and 10 *FH* mutations confirmed by somatic sequencing of the tumors (see Supplementary Table 2 for details).

## Gross Features

All RMCs were centered in the medulla or variably involved it, and 69% (22/32) of the tumors were ill-defined (non-circumscribed) (Figs. 2A–B). Of the CDCs, 41% (14/34) of the tumors were centered in the medulla (Fig. 2C), and 44% (15/34) were large masses involving both the medulla and the cortex. Fifteen percent of CDCs (5/34) were predominantly cortex-based grossly; however, all other tumors microscopically involved the collecting system. Seventy-eight percent of CDCs (25/32) had infiltrative borders, and 22% (7/32) were fairly well-defined, but microscopically showed irregular borders between the tumor and the normal renal parenchyma (Fig. 2D). In FH-deficient RCCs, 20% (5/24) were cortical, 13% (3/24) medullary, and 67% (16/24) were large masses involving both regions. Fifty percent of the tumors (11/22) were described as poorly circumscribed (Fig. 2E); 41% (9/22) were circumscribed and 9% (2/22) were cystic or multicystic. In some cases, multiple benign cystic lesions were observed in adjacent uninvolved renal parenchyma (Fig. 2F). Renal vein invasion was grossly identified in all three subtypes ranging from 30% (7/23) to 44% (14/32).

## Histologic Findings

**Morphologic Patterns of RMC—**Macroscopic and microscopic data are summarized in Table 2. The morphology of individual RMC frequently consisted of mixed patterns. The pattern of solid sheets/cords/nests was seen in 97% (32/33) (primary pattern: 61%; 20/33) (Fig. 3A). Neoplastic cells with rhabdoid features were seen in 30% (10/33) of cases (Fig. 3B) in the poorly differentiated areas. Other commonly observed patterns included: sieve-like or cribriform in 88% (29/33) (primary pattern: 18%; 6/33) (Fig. 3C), reticular pattern reminiscent of the testicular yolk sac tumor (YST) in 85% (28/33) (primary pattern: 9%; 3/33) (Fig. 3D), and tubulopapillary pattern in 36% (12/33) (primary pattern: 12%; 4/33) (Fig. 3E). Sieve-like morphology was usually associated with areas showing reticular pattern. Intracystic pattern (Fig. 3F) and infiltrating glandular patterns (Fig. 3G) were identified as only minor components in 15% (5/33) and 55% (18/33) cases, respectively.

Micropapillary formations without fibrovascular cores were commonly identified in the intracystic pattern (Fig. 3F). Multinodular infiltrating papillary and tubulocystic patterns were not found in any cases. Stromal myxoid change was noted significantly more frequently in RMC compared to other subtypes ($p < 0.0167$). Sickled erythrocytes were visible within the tumor and in the adjacent renal tissue in all cases (Fig. 3H).

**Morphologic patterns of CDC—**CDCs showed mainly interstitial growth patterns with preserved glomeruli (Fig. 4A). Several architectural patterns were commonly seen: solid sheets/cords/nests in 95% (36/38) (primary: 18%; 7/38) (Fig. 4B), tubulopapillary in 84% (32/38) (primary: 37%; 14/38) (Fig. 4C), and infiltrating glandular pattern in 74% (28/38) (primary: 21%; 8/38), with small or medium sized elongated tubules infiltrating in a desmoplastic stroma (Fig. 4D). Multinodular infiltrating papillary growth was seen in 26% (10/38) (primary: 24%; 9/38), comprised by varying sized infiltrating nodules with papillary architecture present in a desmoplastic stroma (Fig. 4E). Sieve-like/cribriform, intracystic papillary, and reticular/YST-like patterns were identified as only minor components in 39% (15/38), 16% (6/38) and 8% (3/38), respectively. Intracystic patterns in CDC demonstrated delicate fibrovascular cores (Fig. 4F), and hyalinization of the cores was observed in 33% (2/6). Tubulocystic pattern was not seen in any case. Dysplastic in situ change of adjacent collecting ducts and sarcomatoid change were observed in 42% (16/38) and 29% (11/38), respectively. (Fig. 4G–H).

**Morphologic patterns of FH-deficient RCC—**The morphologic appearances in this subtype were variable and displayed multiple architectural patterns: tubulopapillary in 86% (25/29) (primary: 38%; 11/29) (Fig. 5A), solid sheets/cords/nests in 79% (23/29) (primary: 24%; 7/29) (Fig. 5B), tubulocystic in 66% (19/29) (primary: 14%; 4/29) (Fig. 5C), intracystic papillary in 55% (16/29) (primary: 3%; 1/29) (Fig. 5D), infiltrating glandular in 48% (14/29) (primary: 3%; 1/29) (Fig. 5E) and multinodular infiltrating papillary in 10% (3/29) (primary: 10%; 3/29) (Fig. 5F). In 50% of the cases (8/16), the intracystic papillary component showed hyalinized fibrovascular cores. Sieve-like/cribriform pattern was often seen as a minor component, present in 62% (18/29) (Fig. 5G). Reticular/yolk sac-like pattern was rarely seen (3%: 1/29) as a tertiary component. Coagulative necrosis was rare in FH-deficient RCC. Of particular note, in this cohort, 13 out of 51 cases (25%) initially contributed as potential CDC were re-classified into FH-deficient RCC, based on FH and 2SC IHC evaluation. Although tubulocystic pattern was not identified in CDC and RMC, 77% (10/13) cases of FH-deficient RCC, initially diagnosed as CDC, demonstrated identifiable tubulocystic component on careful review.

## Immunohistochemical Findings

IHC data are summarized in Table 3 and positive staining patterns are illustrated in Figure 6. The expression of PAX8 and S100A1 in the three categories was 94% (34/36)-97% (26/27) and 82% (23/28)-97% (32/33), respectively. Complete loss of SMARCB1 (INI1) was found in all RMC (as per classification criteria), while SMARCB1 expression was retained in all CDC and FH-deficient RCC. OCT3/4 was expressed in 39 % (13/33) cases of RMC, however diffuse expression (3+) was only seen in 6% (2/33); OCT3/4 expression was completely negative in all CDCs and FH-deficient RCC. Similarly, as per classification

criteria, complete loss of FH and induction of 2SC was seen in FH-deficient RCC, except for 2 cases with equivocal FH findings, in which strong/diffuse nucleocytoplasmic 2SC positivity, and *FH* mutations were detected by sequencing of the tumors. Retained or equivocal FH expression with negative 2SC staining was seen in all CDC and RMC.

### Comparing morphological patterns amongst three groups

A Venn diagram is illustrated in Figure 7, based on the results of the analysis of two tumor subtypes, using the parameters that are statistically different between the 3 groups (detailed in Supplementary Table 1). Sieve-like/cribriform and reticular/YST-like patterns favored RMC, whereas intracystic papillary and tubulocystic patterns favored FH-deficient RCC. Tubulopapillary pattern overlapped in CDC and FH-deficient RCC, while a multinodular infiltrating papillary pattern favored CDC. Infiltrating glandular and solid sheets/cords/nested patterns were not statistically different amongst the three groups.

Grades across all three categories were consistent with ISUP/WHO nucleolar grade 3 or 4 without significant difference amongst these groups ($p$=0.475). Viral inclusion-like large eosinophilic nucleoli with perinucleolar clearing were seen significantly more frequently in FH-deficient RCC, compared to the other groups ($p$<0.0167) (Fig. 5H), while being only focal in RMC and CDC (Figs. 3B, 4D). Regarding the sarcomatoid change (Fig. 4H), there was no significant difference between the subtypes ($p$=0.388).

## DISCUSSION

In this comparative cohort of tumors with morphology as has been associated with high grade distal nephron-related adenocarcinomas, we attempted to ascertain distinguishing clinico-pathological features between RMC, CDC and FH-deficient RCC using clinical, morphologic, and IHC data. Since the time of the previous, largest cohort of CDC and RMC by Gupta et al.,[7] the classification of renal epithelial neoplasms has evolved substantially, particularly with reference to FH-deficient RCC, which must be distinguished from CDC and RMC despite overlapping morphology.[4,8–10,17] First, we acknowledge limitations to the study, most especially its retrospective design, referral basis as source of potential selection bias, and vagaries of sampling related to the variable number of blocks and slides evaluated. Yet, we note these concerns did not prevent ascertainment of statistically significant differences in prevalence and extent of patterns between these groups. Overall, we interpret our findings as suggestive that in many cases differences in histologic patterns between these tumors types are sufficiently characteristic to help guide prospective diagnostic practice, at a minimum for purposes of triage for confirmatory clinical, immunohistochemical, or molecular studies.

RMC has been previously described as a highly aggressive form of RCC occurring in children or young adults of African ancestry with sickle cell trait or disease, and the clinical findings in this study were in line with the previous cohorts,[1–4,7] including individuals of not only African, but also Central and South American and Mediterranean origin.[24] While in many of our cases history of or laboratory evidence of hemoglobinopathy was available, sickle-shaped erythrocytes (drepanocytes) were visible diffusely in all RMC cases included in this study. Securing pertinent history and/or laboratory studies and a careful search for

diffuse sickling within the tumor stroma and blood vessels remain important for this diagnosis.

However, in recent years and since our prior Gupta et al. series[7], two useful IHC biomarkers for RMC have been reported.[25–27] Consistent with recent studies implicating inactivation of *SMARCB1* (INI1, a chromatin remodeling gene on chromosome 22), in the pathogenesis of RMC, increasing experience documents that absent expression of SMARCB1 protein is characteristic of RMC.[25,26] For this reason, absent expression of SMARCB1 was deemed an inclusion criterion in our cohort. Another study showed aberrant expression of OCT3/4 (POU5F1, a transcription factor involved in stem cell phenotypes) in 71% (10/14) of RMCs.[27] In our cohort, positivity for OCT3/4 was seen in 39% (13/33), though diffusely only in 6%. Since CDC and FH-deficient RCC were completely negative, expression of OCT3/4 may have a supporting role in supporting an RMC diagnosis, though overall we regard SMARCB1 as most useful. We do note that previous studies have shown loss of SMARCB1 expression in up to 15% of CDC,[25,28] though the clinical and genetic basis of this observation, especially in an expanding anatomic spectrum of SMARCB1-negative neoplasia,[29] remains unclear. For us, careful assessment for hemoglobinopathy, in an appropriate gross, morphologic, and immunohistochemical context is paramount to diagnosis. This is especially so given our recent experience with a small series of rare tumors with RMC-like histology, SMARCB1 deficient immunophenotype, and aggressive clinical features, arising in individuals where sickle cell trait or disease has been rigorously excluded.[30] Greater study will be necessary to understand the proper classification of such tumors, but presently we designate such tumors as *RCC, unclassified, with medullary phenotype*.[22,30]

From the standpoint of histology, however, our cohort supports the contention that sieve-like/cribriform and reticular/YST-like patterns are prevalent and characteristic in RMC, though by quantitative evaluation we note that they are usually not identified as primary patterns. In contrast, in CDC, tubulopapillary pattern and multinodular infiltrating papillary pattern were observed most frequently, whereas sieve-like/cribriform, reticular/YST-like, and intracystic papillary patterns were only found as minor components. These results are consistent with those previously reported,[1–8] and with the benefit of our experience here, we believe these features can be useful in prospective case triage.

In terms of differentially prevalent histologic patterns, intracystic papillary and tubulocystic patterns, as well as tubulopapillary pattern, were most prevalent and characteristic of the emerging entity of FH-deficient RCC. Regarding the intracystic papillary pattern, 50% of FH-deficient RCC had fibrovascular cores with hyalinization, similar to those reported in the most recent large cohort.[9] On the other hand, micropapillation without fibrovascular cores or delicate fibrovascular cores without hyalinization were predominantly seen in RMC and CDC, though hyalinization of the fibrovascular cores were also observed in 33% of CDC. Hence, in assessing intracystic papillary pattern, hyalinization of fibrovascular cores may be of diagnostic utility, with prominent hyalinization favoring FH-deficient RCC. Regarding the tubulocystic pattern, we note that previous studies on CDC identified this pattern with some frequency.[7,31] However, in the current cohort, in every case studied, CDC-like morphology

with a tubulocystic pattern showed the FH-/2SC+ immunoprofile characteristic of FH-deficient RCC.

We interpret this finding as consistent with our prior findings that tumors showing a pattern of tubulocystic carcinoma with poorly differentiated areas frequently (but certainly not always) represent FH-deficient RCC[10] and further supportive of our recommendations or such cases to undergo workup by IHC and genetic counseling. Finally, we would make note in particular of the issue of the prominent, viral-inclusion like nucleoli with perinucleolar halos characteristic of FH-deficient RCC.[17] These nuclear features were frequent and diffuse in FH-deficient RCC, although they were focally seen in some cases of RMC and CDC. Similar to others,[10,19] we regard the nuclear features to be a sensitive but non-specific feature of FH-deficient RCC, particularly suggestive if present in the morphologic context of the aforementioned intracystic hyalinized papillary or tubulocystic areas.

With respects to the challenging differential between CDC and FH-deficient RCC, our cohort demonstrated that 25% (13/51) of cases previously diagnosed as CDC were re-classified as FH-deficient RCC upon review and use of the contemporary markers, FH and 2SC. Loss of FH and 2SC positivity by IHC have been shown to correlate closely with molecular studies, including *FH* mutations detected from the germline or somatic tumor tissue profiling.[19,32–36] While many emphasize that germline genetic testing is currently the gold standard for HLRCC diagnosis, we urge caution and awareness of the limitations of each molecular technique, given that some individuals may harbor *FH* deletions[10] that may not be detected in many sequencing approaches.[37] Overall, we recommend raising the possibility of FH-deficient RCC based on the histological and cytological features, complemented by IHC as a useful next step to inform triage and recommendation for further genetic counseling. Indeed, one particularly useful aspect of this study is the evaluation of FH and 2SC in a relatively large number of well characterized RMC and CDC compared to prior studies.[9,10,19]

These diagnostic adjuncts are salient because FH-deficient RCCs generally are aggressive tumors.[9,10] In the current series, 75% of patients presented with stage category pT3 or pT4, and 65% died of metastatic disease. We note that all three tumor types behaved in an aggressive fashion and our statistical analyses did not detect a significant difference regarding stage, systemic metastasis or deaths of disease between RMC, CDC and FH-deficient RCC. The most apparent difference, however, pertains to the implication to family members. While RMC remains distinctly rare among individuals with sickle cell trait (and disease), the association of FH-deficient RCC with HLRCC is much more penetrant (~5–20% estimated risk), emphasizing the importance and value of genetic counseling to affected kindreds.

We want to emphasize that before even considering a tumor among this group of high grade, infiltrative renal cell carcinomas, we recommend, foremost, rigorous exclusion of the substantially more prevalent upper tract urothelial carcinomas and metastatic carcinomas, which often show similar infiltrative growth and variable adenocarcinomatous morphology. PAX8 is been known as a reliable renal lineage marker[38,89] yet is expressed in tumors of Müllerian and thyroid origin as well as, usually weakly, a subset of urothelial carcinomas of

the renal pelvis.[40,41] S100A1 has been previously shown to be expressed in common subtypes of renal tumors.[42,43] In the current study, both PAX8 and S100A1 showed high expression in RMC, CDC, and FH-deficient RCC; therefore, the combination of PAX8 and S100A1 may be useful for supporting consideration of renal histogenesis in this setting. Most useful, though, is generous sampling of the pelvicalyceal system to exclude urothelial carcinoma with glandular features.

Finally, we recommend the following algorithm to determine the subtype of high grade distal nephron-related adenocarcinomas. 1) All subtypes of high grade distal nephron-related adenocarcinomas may show some non-specific morphological features such as infiltrating glandular and solid sheets/cords/nested patterns, therefore the possibility of urothelial carcinoma of upper urinary tract and metastatic carcinoma should be excluded. To help confirm renal origin, IHC for PAX8 and S100A1 can be useful. 2) RMC should be diagnosed based on the clinical information (age, race, hemoglobinopathy) and immunohistochemistry (SMARCB1/INI1, OCT3/4), in addition to the sieve-like/cribriform and/or reticular/YST-like morphology. 3) The morphological patterns of tubulopapillary, intracystic papillary and tubulocystic carcinoma-like area with viral inclusion-like macronucleoli with perinucleolar halos suggest the possibility of FH-deficient RCC including HLRCC-RCCs. Since these features overlap with CDC, immunohistochemical combination of FH and 2SC may help in the diagnosis of FH-deficient RCC. 4) A definitive diagnosis of CDC should only be made if RMC and FH-deficient RCC are excluded.

In summary, despite the substantial overlap of morphology of tumors within the spectrum of high grade, infiltrative renal adenocarcinoma, after rigorous histologic evaluation, use of IHC markers, and correlation with clinical findings, reproducible differences in morphology emerge between RMC, CDC and FH-deficient RCC. While we caution that these differences in prevalence and extent of certain morphologic patterns are insufficient to use for diagnosis *per se*, we do argue that they are sufficient in degree to use prospectively for resource conscious triage for confirmatory studies and preliminary interpretation of cases. We also believe that the better understanding of the morphologic range of these cases provided by this study can serve to enable better recognition of these rare aggressive tumors generally, towards the greater end of future studies of their pathogenesis and improved treatment outcomes.

## Supplementary Material

Refer to Web version on PubMed Central for supplementary material.

## ACKNOWLEDGEMENTS:

The authors thank Dr. Santosh Menon, Tata Memorial Hospital, India, for contributing one case of FH-deficient RCC and Dr. Vikas Mehta, Mount Sinai Hospital Medical Center, IL for contributing one case of renal medullary carcinoma.

**Conflicts of Interest and Source of Funding:** S.A.T is supported by the A. Alfred Taubman Medical Research Institute. O.H. acknowledges support of the Charles University Research Fund (project number P36) and by the project CZ.1.05/2.1.00/03.0076 from European Regional Development Fund. C.O. received research fellowship training support from the Uehara Memorial Foundation. Presented in part at the annual meeting of the United States and Canadian Academy of Pathology, Seattle, March, 2016.

## REFERENCES


1. Davis CJ Jr, Mostofi FK, Sesterhenn IA. Renal medullary carcinoma. The seventh sickle cell nephropathy. Am J Surg Pathol. 1995; 19:1–11. [PubMed: 7528470]
2. Swartz MA, Karth J, Schneider DT, et al. Renal medullary carcinoma: clinical, pathologic, immunohistochemical, and genetic analysis with pathogenetic implications. Urology. 2002; 60:1083–1089. [PubMed: 12475675]
3. Watanabe IC, Billis A, Guimaraes MS, et al. Renal medullary carcinoma: report of seven cases from Brazil. Mod Pathol. 2007; 20:914–920. [PubMed: 17643096]
4. Amin MB, Merino MJ. Renal medullary carcinoma. In: Moch H, Humphrey PA, Ulbright TM, et al., eds. WHO Classification. Tumors of the Urinary System and Male Genital Organs. Lyon: IARC; 2016:31–32.
5. Srigley JR, Delahunt B, Eble JN, et al. The International Society of Urological Pathology (ISUP) Vancouver Classification of Renal Neoplasia. Am J Surg Pathol. 2013; 37:1469–1489. [PubMed: 24025519]
6. Karakiewicz PI, Trinh QD, Rioux-Leclercq N, et al. Collecting duct renal cell carcinoma: a matched analysis of 41 cases. Eur Urol. 2007;52:1140–1145. [PubMed: 17336449]
7. Gupta R, Billis A, Shah R, et al. Carcinoma of the collecting ducts of Bellini and renal medullary carcinoma. Am J Surg Pathol. 2012; 36:1265–1278. [PubMed: 22895263]
8. Fleming S, Amin MB, Storkel S. Collecting duct carcinoma. In: Moch H, Humphrey PA, Ulbright TM, et al., eds. WHO Classification. Tumors of the Urinary System and Male Genital Organs. Lyon: IARC; 2016:29–30.
9. Trpkov K, Hes O, Agaimy A, et al. Fumarate hydratase-deficient renal cell carcinoma is strongly correlated with fumarate hydratase mutation and hereditary leiomyomatosis and renal cell carcinoma syndrome. Am J Surg Pathol. 2016;40:865–875. [PubMed: 26900816]
10. Smith SC, Trpkov K, Chen Y-B, et al. Tubulocystic carcinoma of the kidney with poorly differentiated foci: a frequent morphologic pattern of fumarate hydratase-deficient renal cell carcinoma. Am J Surg Pathol. 2016; 40:1457–1472. [PubMed: 27635946]
11. Launonen V, Vierimaa O, Kiuru M, et al. Inherited susceptibility to uterine leiomyomas and renal cell cancer. Proc Natl Acad Sci U S A. 2001; 98:3387–3392. [PubMed: 11248088]
12. Tomlinson IP, Alam NA, Rowan AJ, et al. Germline mutations in FH predispose to dominantly inherited uterine fibroids, skin leiomyomata and papillary renal cell cancer. Nat Genet. 2002;30:406–410. [PubMed: 11865300]
13. Toro JR, Nickerson ML, Wei MH, et al. Mutations in the fumarate hydratase gene cause hereditary leiomyomatosis and renal cell cancer in families in North America. Am J Hum Genet. 2003;73:95–106. [PubMed: 12772087]
14. Wei MH, Toure O, Glenn GM, et al. Novel mutations in FH and expansion of the spectrum of phenotypes expressed in families with hereditary leiomyomatosis and renal cell cancer. J Med Genet. 2006;43:18–27. [PubMed: 15937070]
15. Merino MJ, Torres-Cabala C, Pinto P, Linehan WM. The morphologic spectrum of kidney tumors in hereditary leiomyomatosis and renal cell carcinoma (HLRCC) syndrome. Am J Surg Pathol. 2007;31:1578–1585. [PubMed: 17895761]
16. Lehtonen HJ. Hereditary leiomyomatosis and renal cell cancer: update on clinical and molecular characteristics. Fam Cancer. 2011;10:397–411. [PubMed: 21404119]
17. Merino MJ, Linehan WM. Hereditary leiomyomatosis and renal cell carcinoma–associated renal cell carcinoma. In: Moch H, Humphrey PA, Ulbright TM, et al., eds. WHO Classification. Tumors of the Urinary System and Male Genital Organs. Lyon: IARC; 2016:25–26.
18. Smith SC, Trpkov K, Mehra R, et al. Is tubulocystic carcinoma with dedifferentiation a form of HLRCC/fumarate hydratase-deficient RCC? Mod Pathol. 2015; suppl 2s:260A.
19. Chen YB, Brannon AR, Toubaji A, et al. Hereditary leiomyomatosis and renal cell carcinoma syndrome-associated renal cancer: recognition of the syndrome by pathologic features and the utility of detecting aberrant succination by immunohistochemistry. Am J Surg Pathol. 2014;38:627–637. [PubMed: 24441663]

20. Chen YB, Kong M, Bialik A, et al. Hereditary leiomyomatosis and renal cell carcinoma (HLRCC)-associated renal cancer: a comparison of fumarate hydratase (FH) and S-(2-succino)-cysteine (2SC) immunohistochemistry as ancillary tools. Mod Pathol. 2015;28(suppl 2):211A.
21. Carvalho JC, Thomas DG, McHugh JB, et al. p63, CK7, PAX8 and INI-1: an optimal immunohistochemical panel to distinguish poorly differentiated urothelial cell carcinoma from high-grade tumours of the renal collecting system. Histopathology. 2012; 60:597–608. [PubMed: 22260386]
22. Amin MB, Smith SC, Agaimy A, et al. Collecting duct carcinoma versus renal medullary carcinoma: an appeal for nosologic and biological clarity. Am J Surg Pathol. 2014; 38:871–874. [PubMed: 24805860]
23. Delahunt B, Cheville JC, Martignoni G, et al. The International Society of Urological Pathology (ISUP) grading system for renal cell carcinoma and other prognostic parameters. Am J Surg Pathol. 2013;37:1490–1504. [PubMed: 24025520]
24. John N A review of clinical profile in sickle cell traits. Oman Med J. 2010; 25:3–8. [PubMed: 22125689]
25. Calderaro J, Moroch J, Pierron G, et al. SMARCB1/INI1 inactivation in renal medullary carcinoma. Histopathology. 2012;61: 428–435. [PubMed: 22686875]
26. Liu Q, Galli S, Srinivasan R, et al. Renal medullary carcinoma: molecular, immunohistochemistry, and morphologic correlation. Am J Surg Pathol. 2013; 37:368–374. [PubMed: 23348212]
27. Rao P, Tannir NM, Tamboli P. Expression of OCT3/4 in renal medullary carcinoma represents a potential diagnostic pitfall. Am J Surg Pathol. 2012; 36:583–588. [PubMed: 22301499]
28. Elwood H, Chaux A, Schultz L, et al. Immunohistochemical analysis of SMARCB1/INI-1 expression in collecting duct carcinoma. Urology. 2011;78: e471–e475.
29. Agaimy A The expanding family of SMARCB1(INI1)-deficient neoplasia: implications of phenotypic, biological, and molecular heterogeneity. Adv Anat Pathol. 2014; 21:394–410. [PubMed: 25299309]
30. Sirohi D, Smith SC, Ohe C, et al. Renal cell carcinoma, unclassified with medullary phenotype: poorly-differentiated adenocarcinomas overlapping with renal medullary carcinoma. Hum Pathol. 2017; 67:134–145. [PubMed: 28716439]
31. Amin MB, Varma VD, Tickoo SK, et al. Collecting duct carcinoma of the kidney. Adv Anat Pathol. 1997;4:85–94.
32. Nagai R, Brock JW, Blatnik M, et al. Succination of protein thiols during adipocyte maturation: a biomarker of mitochondrial stress. J Biol Chem. 2007; 282:34219–34228. [PubMed: 17726021]
33. Bardella C, El-Bahrawy M, Frizzell N, et al. Aberrant succination of proteins in fumarate hydratase-deficient mice and HLRCC patients is a robust biomarker of mutation status. J Pathol. 2011;225:4–11. [PubMed: 21630274]
34. Joseph NM, Solomon DA, Frizzell N, et al. Morphology and Immunohistochemistry for 2SC and FH Aid in Detection of Fumarate Hydratase Gene Aberrations in Uterine Leiomyomas From Young Patients. Am J Surg Pathol. 2015;39:1529–39. [PubMed: 26457356]
35. Oteri KL, Linehan MW, Merino MJ. IHC helps to identified renal tumors associated with HLRCC syndrome. Mod Pathol. 2014;27(suppl 2):243A.
36. Smith SC, Sirohi D, Ohe C et al. A distinctive, low-grade oncocytic fumarate hydratase-deficient renal cell carcinoma, morphologically reminiscent of succinate dehydrogenase-deficient renal cell carcinoma. Histopathol. 2017;71(1):42–52.
37. Vocke CD, Ricketts CJ, Merino MJ et al. Comprehensive genomic and phenotypic characterization of germline FH deletion in hereditary leiomyomatosis and renal cell carcinoma. Genes Chromosomes Cancer. 2017;56(6):484–492. [PubMed: 28196407]
38. Laury AR, Perets R, Piao H, et al. A comprehensive analysis of PAX8 expression in human epithelial tumors. Am J Surg Pathol. 2011;35:816–826. [PubMed: 21552115]
39. Reuter VE, Argani P, Zhou M et al. Best practices recommendations in the application of immunohistochemistry in the kidney tumors: report from the International Society of Urologic Pathology consensus conference. Am J Surg Pathol. 2014;38(8): e35–49. [PubMed: 25025368]

40. Ozcan A, Shen SS, Hamilton C, et al. PAX 8 expression in non-neoplastic tissues, primary tumors, and metastatic tumors: a comprehensive immunohistochemical study. Mod Pathol. 2011;24:751–764. [PubMed: 21317881]

41. Tong GX, Yu WM, Beaubier NT, et al. Expression of PAX8 in normal and neoplastic renal tissues: an immunohistochemical study. Mod Pathol. 2009;22(9):1218–1227. [PubMed: 19525927]

42. Li G, Gentil-Perret A, Lambert C, Genin C, Tostain J. S100A1 and KIT gene expressions in common subtypes of renal tumours. Eur J Surg Oncol. 2005;31(3):299–303. [PubMed: 15780567]

43. Rocca PC, Brunelli M, Gobbo S, et al. Diagnostic utility of S100A1 expression in renal cell neoplasms: an immunohistochemical and quantitative RT-PCR study. Mod Pathol. 2007;20(7):722–728 [PubMed: 17483815]

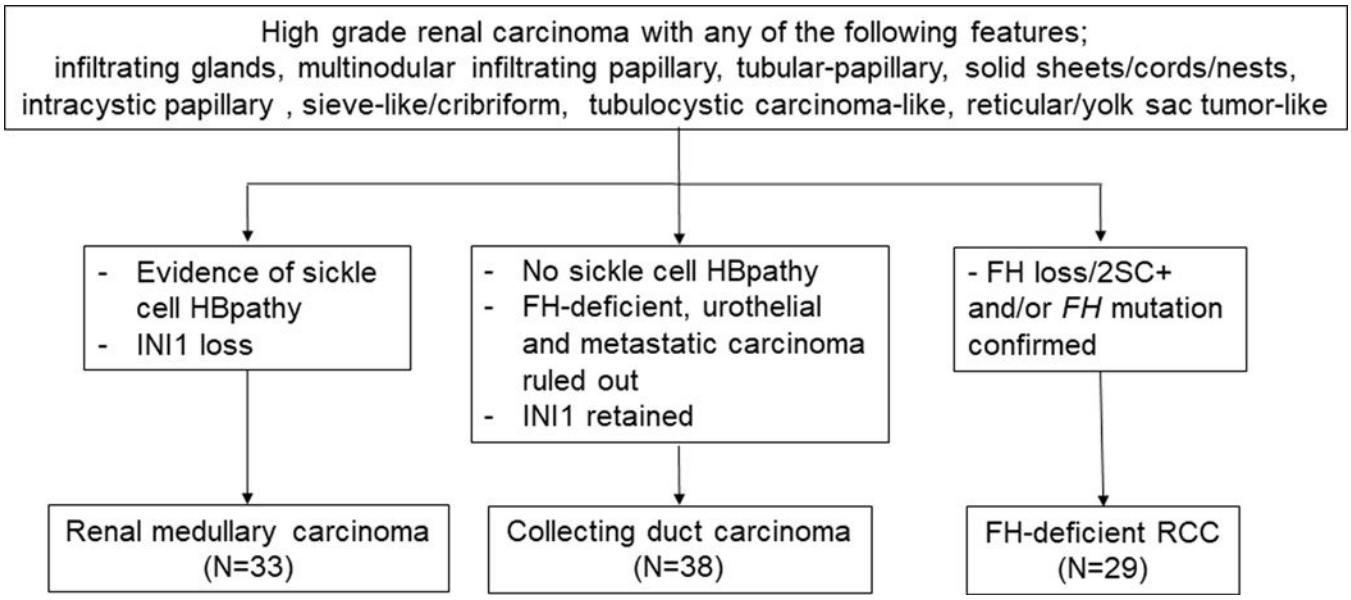


**Figure 1.**
Design of this high-grade distal nephron-related adenocarcinoma study.

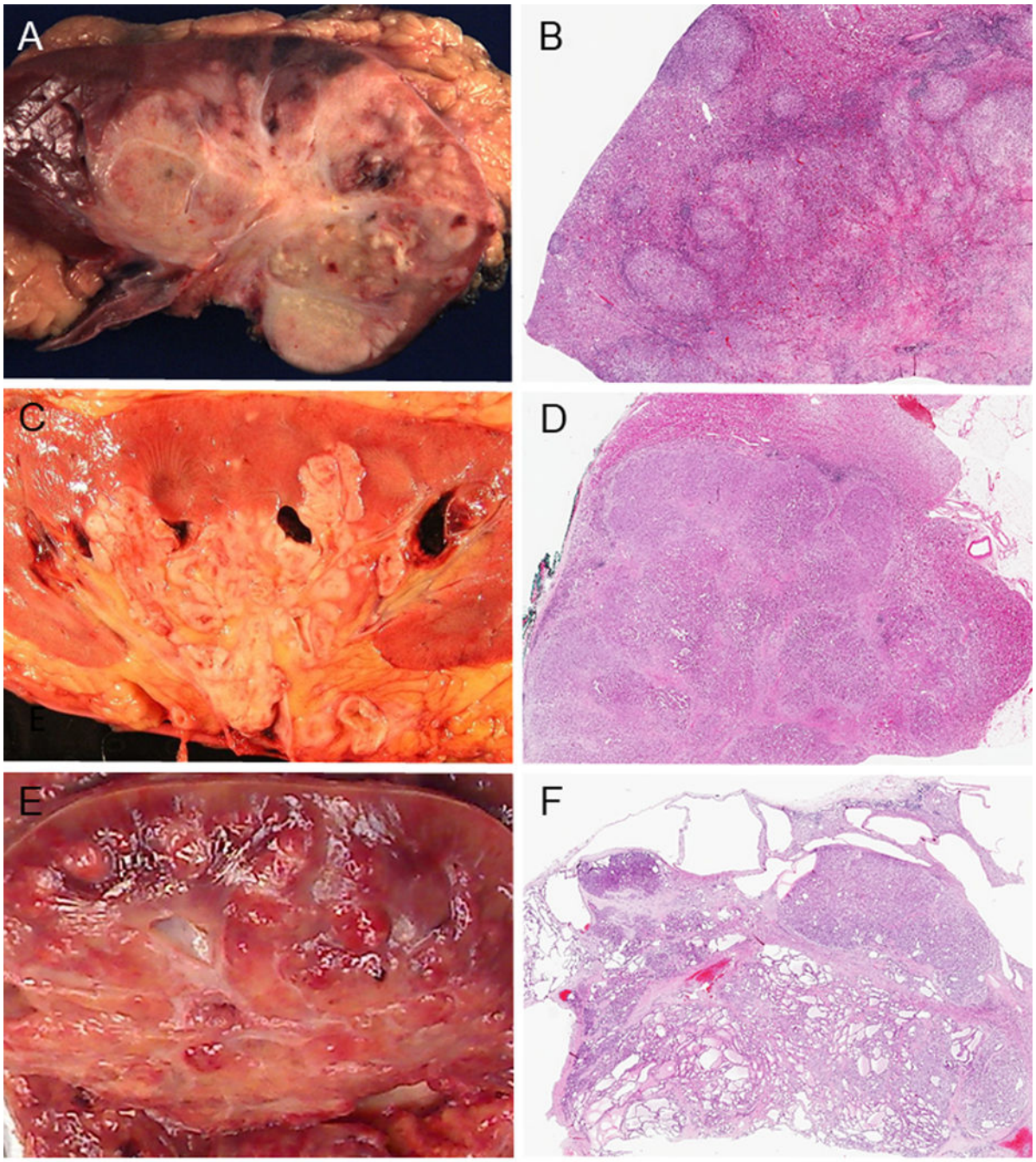


**FIGURE 2.**

Gross features and low power images. Gross features (A, C, E). (A) Renal medullary carcinoma (RMC): poorly circumscribed tumor occupying a large part of the parenchyma. (C) Collecting duct carcinoma (CDC): tumor centered in the medulla. (E) FH-deficient RCC: poorly-defined tumor involving the cortex and medulla. Low power images (B, D, F). (B) RMC: the tumor displays infiltrating irregular border and satellite nodules are seen in the cortex. (D) CDC: the tumor is overall well-defined, but focally invasive. Infiltrating growth pattern is also seen. (F) FH-deficient RCC: The tumor is overall well circumscribed with

tubulocystic pattern. Multiple benign cystic lesions are seen in adjacent uninvolved renal parenchyma.

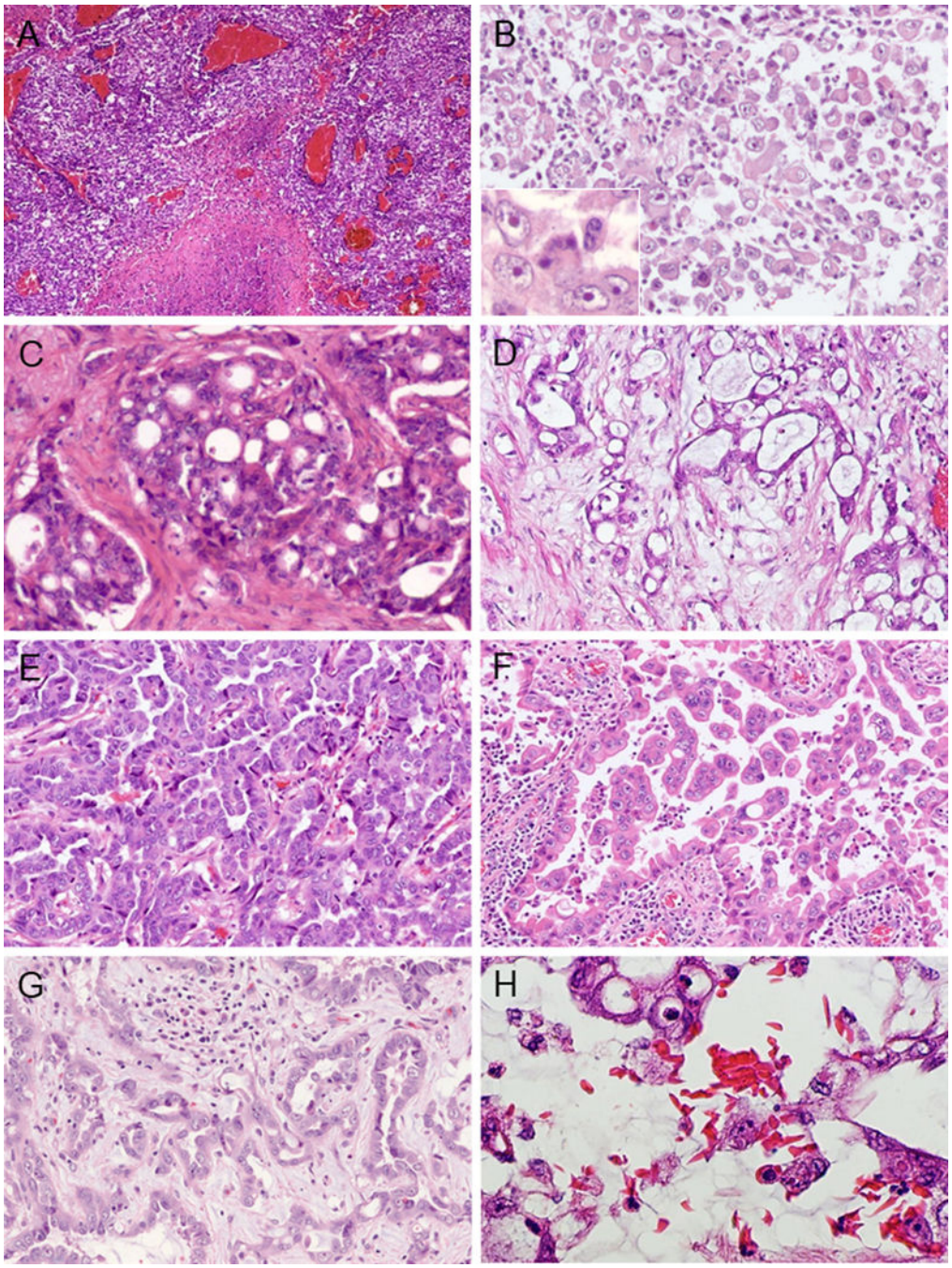


**FIGURE 3.**

Morphological patterns of RMC (A-H). (A) Sheet-like growth pattern with coagulative necrosis. (B) Neoplastic cells showing rhabdoid features. Inset shows prominent nucleoli. (C) Sieve-like/cribriform pattern. Cribriform nests are embedded in the desmoplastic stroma. (D) Reticular/Yolk sac tumor (YST)-like pattern. Tumor cell aggregates of irregular size and shape are seen in loose myxoid stroma reminiscent of testicular YST. (E) Tubulopapillary pattern. (F) Intracystic papillary pattern. Micropapillation without fibrovascular core are

seen in the microcystic space. (G) Infiltrating glandular pattern. Irregular glands are seen infiltrating in myxoid stroma. (H) Sickled erythrocytes are histologically identified.

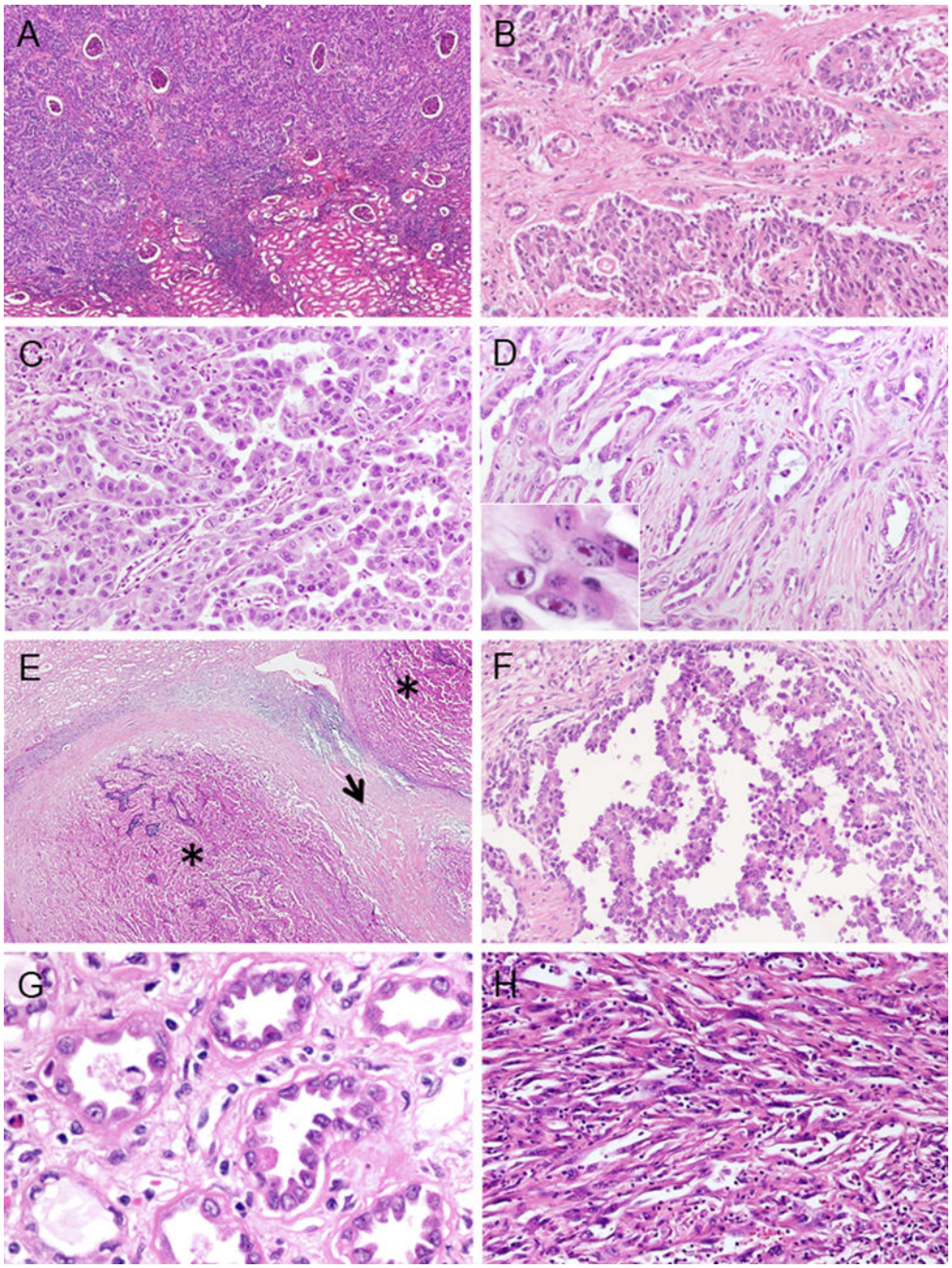


**FIGURE 4.**

Morphological patterns of CDC (A-F). (A) Interstitial infiltrating growth. (B) Solid sheets-nested pattern. (C) Tubulopapillary pattern. (D) Infiltrating glandular pattern. Small or medium sized elongated tubules in desmoplastic stroma. In7set shows prominent nucleoli. (E) Multinodular infiltrating growth pattern. Multiple infiltrative nodules of varying size with papillary architecture (*) and desmoplasia between nodules (arrow). (F) Intracystic papillary pattern with delicate fibrovascular core. Other findings of CDC (G-H). (G) Dysplastic in situ change within adjacent collecting ducts. (H) Sarcomatoid change.

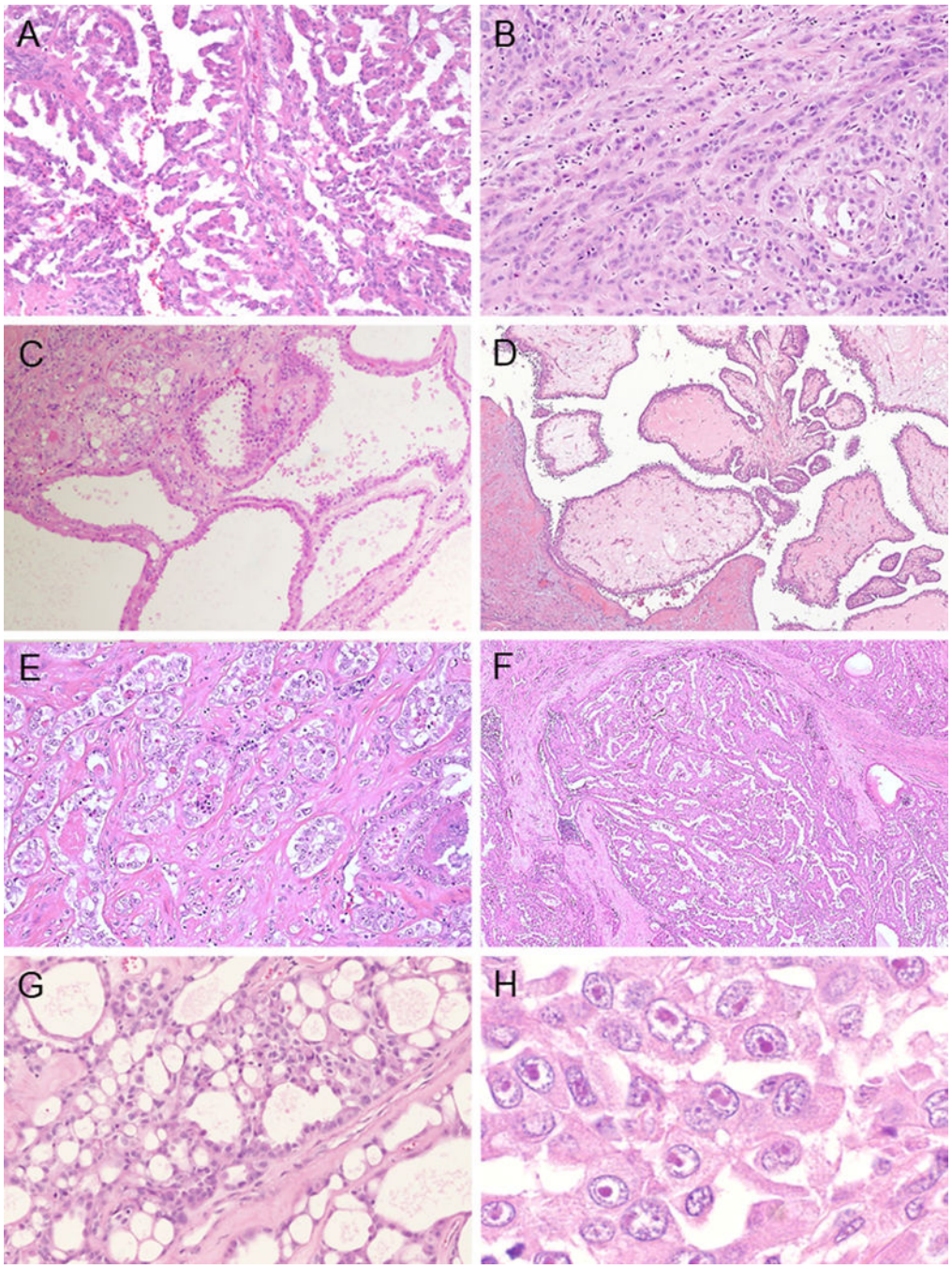


**FIGURE 5.**

Morphological pattern of FH-deficient RCC (A-H). (A) Papillary pattern. (B) Cord-like or small nests architectures. (C) Tubulocystic pattern. Poorly differentiated foci are identified in left upper sides. (D) Intracystic papillary pattern with hyalinized cores. (E) Infiltrating glands within desmoplastic stroma. (F) Multinodular infiltrating papillary pattern. (G) sieve-like nests randomly punctuated by irregular small cystic spaces. (H) Viral inclusion-like nucleoli are frequently seen.

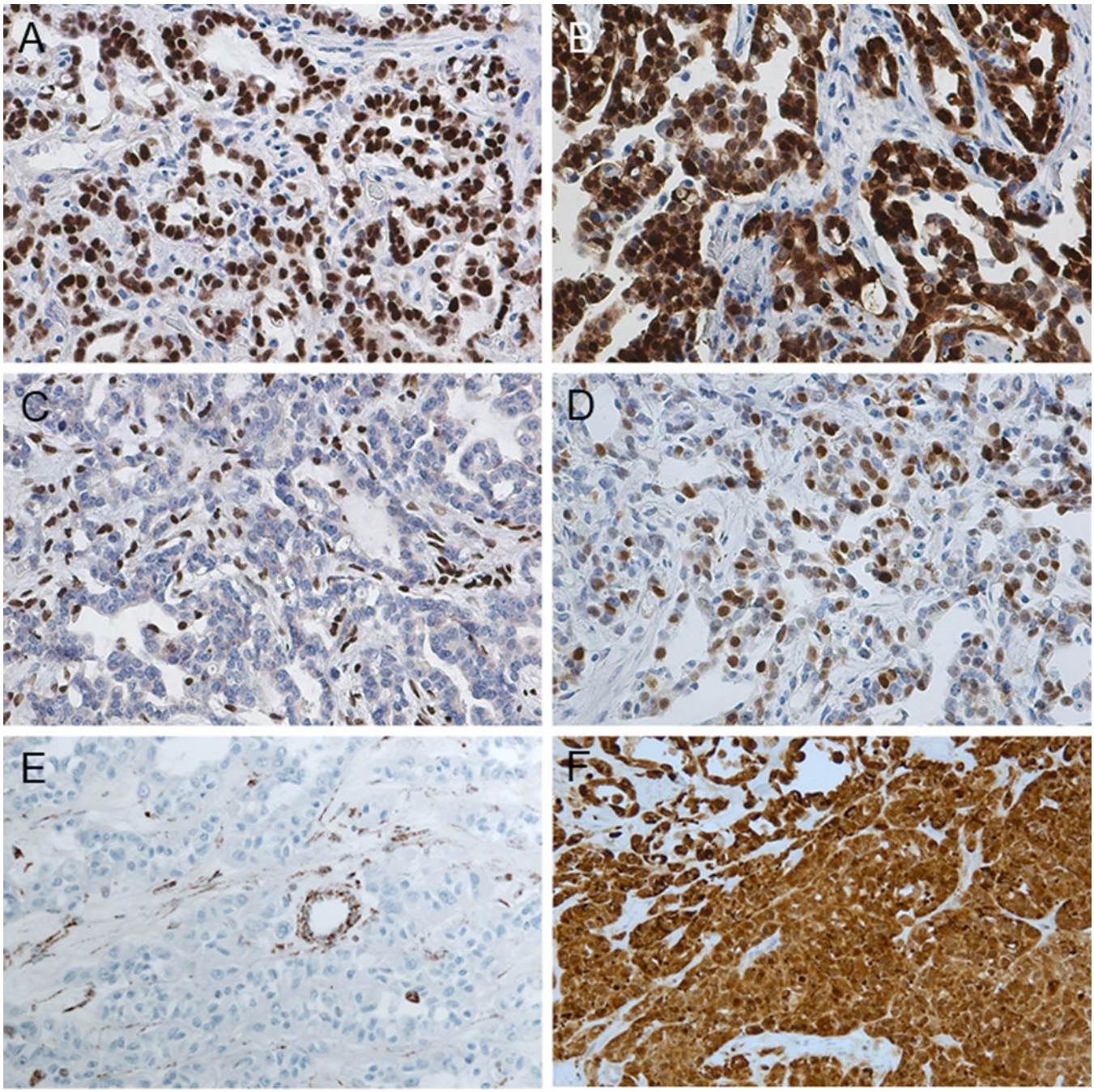


**FIGURE 6.**

Immunohistochemistry (A-F). (A) PAX8: diffuse nuclear positivity. (B) S100A1: diffuse nuclear and cytoplasmic positivity. (C) SMARCB1/INI1: complete loss in tumor cells (internal control shows positive staining). (D) OCT3/4: nuclear positivity. (A-D: RMC) (E) FH: complete loss in tumor cells (internal control shows positive staining). (F) 2SC: strong and diffuse nucleocytoplasmic positivity (E-F: FH-deficient RCC).

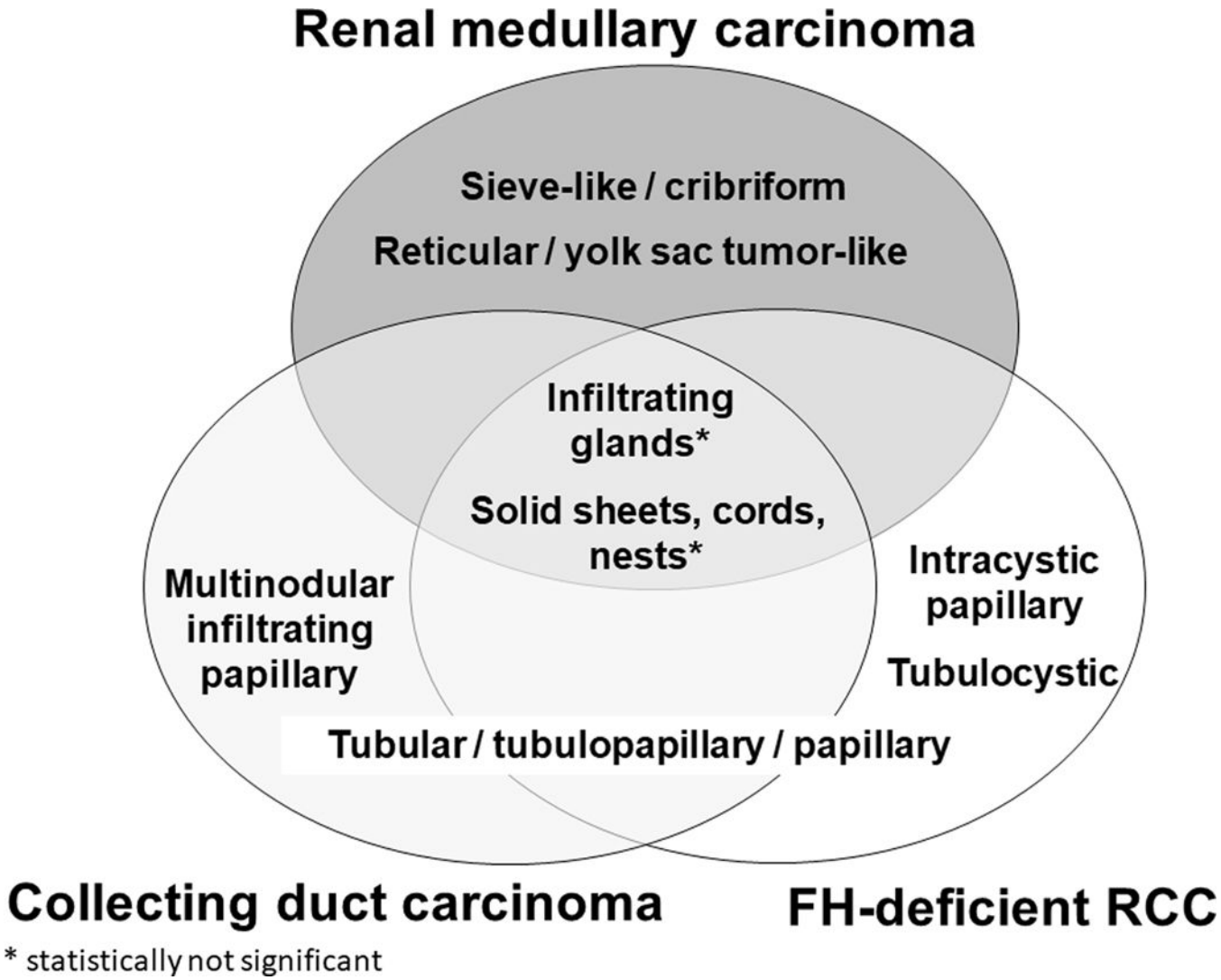


**FIGURE 7.**
Comparison of morphological patterns amongst RMC, CDC and FH-deficient RCC.

**Table 1.**

Clinical features

| | | RMC (n=33) | CDC (n=38) | FH-deficient RCC (n=29) | *p*-value |
|---|---|---|---|---|---|
| Median age (range) | | 27.0 (10–63) | 65.5 (16–83) | 45.0 (18–71) | << 0.001 |
| Male: Female | | 2.6: 1 | 3.2: 1 | 3.1: 1 | 0.958 |
| Race | Caucasian<br>African-American<br>Other | 9% (3/32)<br>78% (25/32)<br>13% (4/32) | 90% (28/31)<br>7% (2/31)<br>3% (1/31) | 71% (17/24)<br>12% (3/24)<br>17% (4/24) | NA |
| Sickle cell disorder | | 100% * | 0% | 0% | NA |
| Family history of HLRCC or RCC (H) / HLRCC stigmata (S) | | 0% | 0% | H: 39% (7/18)<br>S: 29% (5/17) | NA |
| Laterality ** | | 75% (24/32) | 44% (14/32) | 43% (12/28) | < 0.0167 |
| Tumor size cm (range) | | 6.4 (4–12) | 6.3 (2–15.8) | 8.5 (3–18) | < 0.05 |
| pT stage category | pT1–2<br>pT3–4 | 15% (5/33)<br>85% (27/33) | 9% (3/34)<br>91% (31/34) | 25% (7/28)<br>75% (21/28) | 0.225 |
| Local recurrence | | 14% (4/29) | 23% (5/22) | 15% (3/20) | 0.723 |
| Lymph node metastasis | | 96% (25/26) | 48% (13/27) | 58% (15/26) | < 0.0167 |
| Systemic metastasis | | 94% (30/32) | 73% (16/22) | 65% (17/26) | 0.0169 |
| Metastasis at presentation | | 70% (19/27) | 47% (7/15) | 46% (6/13) | 0.194 |
| Dead of disease<br>mean time to death (month); range | | 83% (24/29) 10.3;<br>7days– 25 | 61% (14/23)<br>11.6;<br>2.5– 37 | 61% (14/23)<br>18.6;<br>2– 64 | 0.145 |

* The history of sickle cell trait sickle cell hemoglobinopathy was unavailable in 18% (6/33), however, histological sickled erythrocytes were seen.

** predilection for right kidney. NA, not analyzed.

**Table 2.**

Macroscopic and microscopic features

| | RMC | CDC | FH-deficient RCC | *p*-value |
|---|---|---|---|---|
| Macroscopic features | | | | |
| Location; medulla cortex & medulla | 56% (18/32)<br>44% (14/32) | 41% (14/34)<br>44% (15/34) | 13% (3/24)<br>67% (16/24) | NA |
| Infiltrating border | 69% (22/32) | 78% (25/32) | 50% (11/22) | 0.110 |
| Renal vein invasion | 41% (13/32) | 44% (14/32) | 30% (7/23) | 0.669 |
| Microscopic features | | | | |
| #1 (infiltrating gland) | 55% (18/33) | 74% (28/38) | 48% (14/29) | 0.0775 |
| #2 (MIP) | 0% (0/33) | 26% (10/38) | 10% (3/29) | < 0.0167 |
| #3 (tubular, papillary) | 36% (12/33) | 84% (32/38) | 86% (25/29) | < 0.0167 |
| #4 (solid sheet, cord, nest) | 97% (32/33) | 95% (36/38) | 79% (23/29) | 0.436 |
| #5 (intracystic papillary) | 15% (5/33) | 16% (6/38) | 55% (16/29) | < 0.0167 |
| #6 (sieve-like/cribriform) | 88% (29/33) | 39% (15/38) | 62% (18/29) | < 0.0167 |
| #7 (tubulocystic) | 0% (0/33) | 0% (0/38) | 66% (19/29) | < 0.0167 |
| #8 (reticular/YST-like) | 85% (28/33) | 8% (3/38) | 3% (1/29) | < 0.0167 |
| HLRCC-like nucleoli<br>(1+; 2+) | 39% (13/33)<br>(30%; 9%) | 40% (15/38)<br>(29%; 11%) | 100% (29/29)<br>(21%; 79%) | < 0.0167 |
| Coagulative necrosis | 64% (21/33) | 68% (26/38) | 17% (5/29) | < 0.0167 |
| Dysplastic in situ change | 6% (2/33) | 42% (16/38) | 11% (3/28) | < 0.0167 |
| Stromal myxoid change | 94% (31/33) | 26% (10/38) | 39% (11/28) | < 0.0167 |
| Sarcomatoid change | 15% (5/33) | 29% (11/38) | 28% (8/19) | 0.388 |
| ISUP/WHO grade 3, 4 | 58% (19/33),<br>42% (14/33) | 63% (24/38),<br>37% (14/38) | 72% (21/29),<br>28% (8/29) | 0.475 |

MIP; multinodular infiltrating papillary, YST: yolk sac tumor

**Table 3.**

Immunohistochemistry

| | | RMC | CDC | FH-deficient RCC |
|---|---|---|---|---|
| PAX8 | (+) | 97% (32/33) | 94% (34/36) | 97% (26/27) |
| S100A1 | (+) | 97% (32/33) | 94% (34/36) | 82% (23/28) |
| SMARCB1/INI1 | (loss) | 100% (33/33) | 0% (0/37) | 0% (0/25) |
| OCT3/4 | (+) | 39% (13/33) * | 0% (0/37) | 0% (0/26) |
| FH | (+)<br>(+/−)<br>(−) | 97% (32/33)<br>3% (1/33)<br>0% (0/33) | 84% (32/38)<br>16% (6/38)<br>0% (0/38) | 0% (0/29)<br>7% (2/29)<br>93% (27/29) |
| 2SC | (+)<br>(−) | 0% (0/1)<br>100% (1/1) | 0% (0/13)<br>100% (13/13) | 100% (25/25)<br>0% (0/25) |

* 1+;15%, 2+;18%, 3+;6%